CLINICAL DOSIMETRY TOOL IMPLEMENTATION OF I-131 MIBG THERAPY
FOR PHEOCHROMOCYTOMA AND PARAGANGLIOMA

By

Roberto C. Perez Franco

A THESIS

Presented to the Departments of Medical Physics and Diagnostic Radiology
and the Oregon Health & Science University
School of Medicine
in partial fulfillment of
the requirements for the degree of

Master of Science

June 2020

School of Medicine
Oregon Health & Science University

CERTIFICATE OF APPROVAL
This is to certify that the Master's thesis of
Roberto C. Perez Franco
has been approved

_____
Andrei Pugachev, Ph.D. (Mentor/Advisor)

_____
Lindsay DeWeese, Ph.D. (Chair)

_____
Thomas Griglock, Ph.D. (Member)

Table of Contents

Acknowledgements

I would like to express my sincere gratitude the medical physics faculty and the hospital staff at Oregon Health & Science University for their instructive help in both academic and clinical settings. In particular, I would like to thank the members of my thesis advisory committee. First, I want to thank my advisor, Dr. Andrei Pugachev, for introducing me to this unique project, patiently guiding me through the research process, being available to answer my questions, and most importantly encouraging me throughout entirety of this project. Second, I would like to thank both Dr. Lindsay DeWeese and Dr. Thomas Griglock, for their didactic and clinical guidance in the diagnostic realm of medical physics.

Furthermore, I would like to thank my fellow students: Aaron, Amanda, Ze, Austin, Connor, as well as the students who preceded and succeeded us in the program for their support and friendship in the past two years.

Lastly, I would like to thank my parents, siblings and other family members down in Guatemala for believing in me, supporting me, and taking care of me all my life. Especially in the past couple of years that I have been completing my bachelor's and master's degrees.

Abstract

Purpose: To calculate a therapeutic activity for safe administration of Iodine-131 MIBG in patients undergoing the AZEDRA therapy [1] by ensuring that the radiation dose limits are not exceeded for critical organs.

Methods: A tool for image analysis and dosimetry was developed based on the guidelines set of the AZEDRA dosimetry protocol. The tool was designed to process count data obtained from regions of interest drawn in three planar gamma camera images obtained over a period of 72 hours. Using the count data for the ROIs organ activities were calculated and fitted with a mono-exponential curve to obtain the cumulated activity within those regions. The estimates of radiation dose to each of the relevant organs at risk (kidneys, liver, lungs) were evaluated using a software employing the MIRD methodology. More specifically, the doses to these organs were calculated using OLINDA/EXM® software [2] and imported into the spreadsheet. To account for each patient's unique anatomy, the organ masses were obtained from volumetric measurements of a CT scan. The nominal therapeutic activity of 1000 mCi (injected in two sessions) was scaled down, when needed, as to ensure that organs at risk did not exceed the limits.

Results: The finished tool was used for the analysis of two patients' scans. The quantitation of the image data showed that the individual organ uptake and biological excretion rate were patient-dependent. Therefore, the maximum therapeutic activity varied between patients due to the differences in the clearance rate, organ uptake and tumor burden.

Conclusions: The implementation of this image analysis and dosimetry tool allows for a streamlined performance of patient-specific organ dose estimation, and therapeutic activity calculation. The tool has proven to be clinically useful in determining dose estimates to the OARs of two patients who have already been successfully treated.

1. Introduction

Cancer treatments vary with respect to the anatomy to be treated. For instance, chemotherapy is widely used for cancers that reside in the blood or that have metastasized into the lymphatic system while radiation therapy can be used more selectively to target different neoplasms throughout the body. Additionally, cancers can also be treated by using radiopharmaceuticals [3]. This type of treatment can be considered a hybrid of the other two methods. This is because the radiopharmaceuticals are chemically designed to target a specific anatomy or metabolic process within the body and deliver a substantial radiation dose.

An example of one such radiopharmaceutical is Metaiodobenzylguanidine (MIBG) also known as Iobenguane was developed in the late 1970s at the Michigan University Medical Center for imaging of the adrenal medulla and a wide range of tumors of neural crest origin [4]. More specifically, it can be used in the evaluation of pheochromocytomas and paragangliomas when it is labeled with iodine-123 and allows one to assess the potential for patients to be treated with iodine-131 [5] [6].

The decay of iodine-123 permits it to be used in diagnostic imaging as it decays by electron capture into Te-123 which subsequently releases of 159 keV gamma rays [7]. These gamma rays can be efficiently detected by gamma cameras in planar or single photon emission computed tomography (SPECT) mode [8]. These imaging modalities can produce images in two and three dimensions respectively. Iodine-131 can be used for therapy purposes as it primarily decays by emitting beta particles and gammas rays. The decay starts from the division of a neutron into a proton, an electron (beta particle), a neutrino

and energy. The new nucleus of the atom has an extra proton and some energy left i.e. a metastable Xenon atom. The beta particles emitted from the nucleus interact with surrounding matter and deposit their energy in very small distances, in the order of tens of millimeters [9]. The newly formed, metastable Xenon isotope decays by gamma ray emission Thus leaving a stable Xenon-131 atom behind while the gamma ray can be imaged by the aforementioned gamma cameras. Though the light-photons could be detected by using a standard camera, for the detection of higher energy photons a dedicated gamma camera is needed. The cameras are manufactured with thicker crystals in order to stop the high energy photons and improve the detection efficiency.

It is possible to diagnose and then treat patients by only using radiopharmaceuticals labeled with Iodine-131. Iodine-123, while being chemically identical to Iodine-131 decays by electron capture to Tellurium-123 and emits gamma photons with a dominant energy of 159 keV, so Iodine-123 cannot be used for therapeutic applications, but it can be very well-suited for diagnostic imaging applications [7]. However, while I-123 MIBG can be used to localize the areas of interest, this isotope does not provide the same physiological information that I-131 does due to the fact that their half-lives are not the same. Iodine-123 has a half-life of 13 hours while Iodine-131 has a half-life of 8.02 days. The activity residence time can be determined for each patient as a result of imaging with I-131 [10] [7].

The methods used for the production of these two radioisotopes also differ. Iodine 123 is produced in a cyclotron by using xenon as a base element. On the other hand, I-131 is a byproduct of fission. Relaying in the coordinated production of two radioisotopes and

the subsequent labeling of the MIBG compound complicates the workflow and can potentially create a bottle neck.

Therefore, there are certain advantages to using a single radiopharmaceutical to image and treat the patients. For instance, I-131 MIBG/AZEDRRA therapy protocol as developed by Progenics Pharmaceuticals Inc. was approved for clinical use by the FDA in 2018 [11]. The AZEDRA therapy began in the nuclear medicine department at Oregon Health & Science University (OHSU) in late 2019. Its first clinical use, in November of 2019, required the implementation of the radionuclide therapy dosimetry protocol. The purpose of the dosimetry calculation is to ensure that radiation dose limits to the critical OARs (liver, lungs and kidneys) are not exceeded after injecting the patients with the therapeutic amounts of Iodine-131 MIBG activity which can be as high as 1000 mCi due to hematologic toxicity [12].

The dosimetry protocol that was implemented with this research utilizes the data collected from regions of interest to calculate the cumulated activity for all relevant organs. Then, the cumulated activity and organ masses are inputted into an external software called OLINDA/EXM® [2] to calculate the doses to the OARs. Thereafter, the organ doses are imported back into the image analysis tool to calculate a safe therapeutic activity. Thus, patients suffering from pheochromocytomas or paragangliomas can be safely treated with the I-131 AZEDRA MIBG radiopharmaceutical therapy.

2. Background

2.1. Detecting Cancer with Radiopharmaceuticals

2.1.1. Radioactive Decay

Unstable elements spontaneously decay into other elements with smaller nuclei (daughters), atomic particulate (alpha, beta, positron, etc.) and energy in the form of photons (gamma rays) [13] [14]. In the case of gamma rays, mass is converted into energy. These transitions towards a lower energy state can be combinations of these spontaneous decays, but they are unique to each individual radioisotope. Therefore, in the interest of time, the types of decay that will be discussed next are the ones that pertain to this research. More specifically, the decay scheme of iodine-131, which consists of a beta decay followed by an isomeric transition or gamma emission.

2.1.2. Beta Emission (β^-)

This emission occurs when a neutron in the nucleus of an unstable element is transformed into a proton, an electron, a neutrino and energy,

$$n \rightarrow p^+ + e^- + \nu + enery \qquad (Eq.\,2.\,1)$$
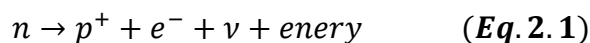
This type of decay is particularly important in the treatment of cancer because electrons can lose their energy by transferring it into matter [13]. This is due to the fact that electrons have an intrinsic negative charge and primarily interact with the matter by Coulombic forces. Additionally, the energy of the electron as it exits the nucleus is also an important factor to consider. More specifically, a highly energized electron can ionize atoms and molecules for longer distances than one with low kinetic energy [9] [15]. The ionization can alter the DNA structure of the tissue. The DNA has mechanisms to repair itself, but if

4

it does not repair itself correctly the cell dies or passes on a mutation when it reproduces. The most lethal lesion to DNA is a double strand break because these are often not repaired or are poorly repaired leading to cell death or DNA mutation respectively [16] [17]. Of course, this happens to all tissues indiscriminately. Therefore, it is important to ensure that the radiation dose is delivered primarily to cancerous tissue.

2.1.3. Isomeric Transition or Gamma Ray Emission

This type of emission occurs when the nucleus of an atom has excess energy after it has become a daughter from another type of decay [13]. This process competes with another decay mode called internal conversion. As the photon exits the atom radius, it can interact with an electron in the atom outer shells, which it can eject if it has enough energy. Nevertheless, if a gamma ray makes it out of the atom, it can be detected by a gamma camera and used for diagnostic imaging.

Iodine 131 decays in by multiple modes. Two of these modes can be considered dominant. There is a total of 970.8 keV available for the radioactive I-131 to give up as it transitions into a stable Xenon 131 atom. The energy of the beta particle emitted varies and the energy of the gamma ray(s) changes with it. Figure 2.1 illustrates a few of the different possible outcomes of the spontaneous decay of the radioactive iodine atom. Furthermore, the chance of occurrence for each of these events is listed as a probability. All events start with beta particles being emitted to form a metastable Xenon 131 which consequently decays by emitting a gamma ray. For instance, the most probable energy of the beta particle is 606.3 keV (89.6%), and the most probable energy for the gamma ray is 364.5 keV (81.5%) [18].
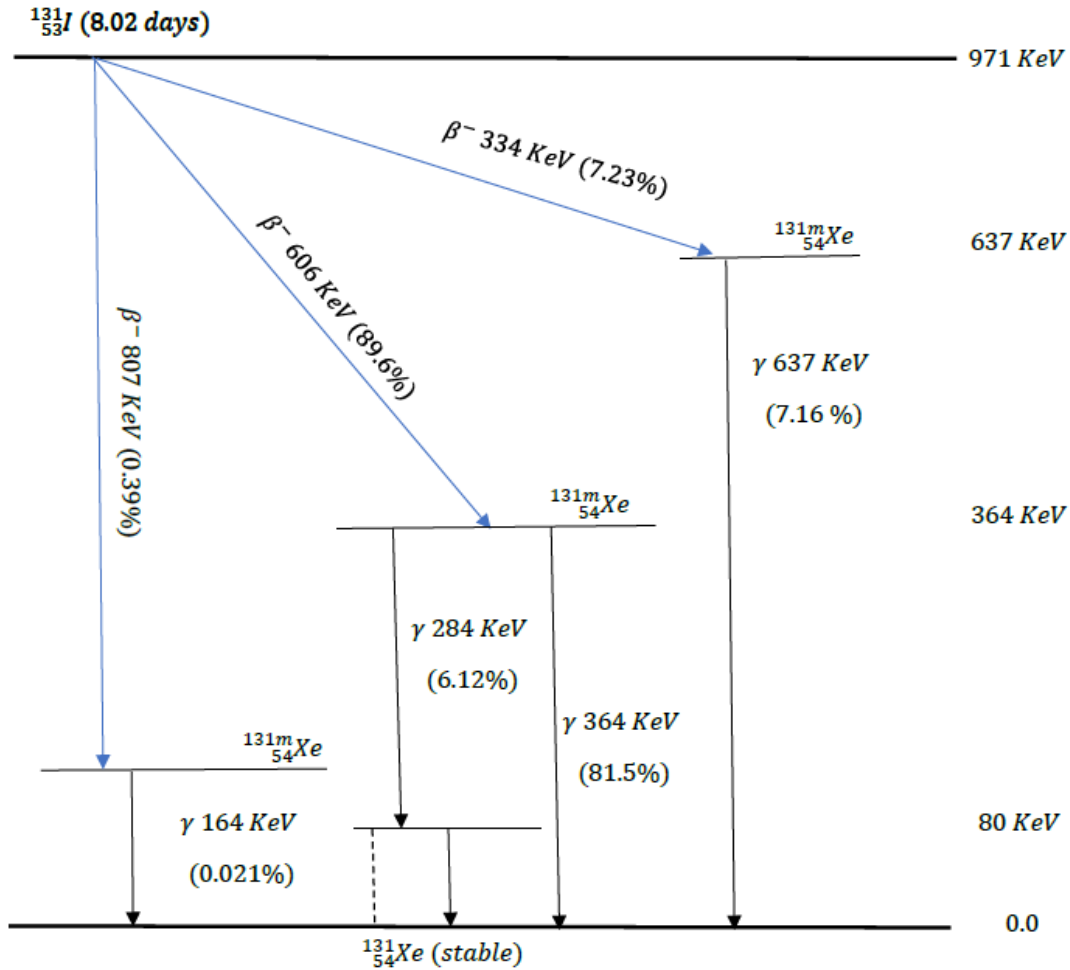
Figure 2.1. Iodine 131 decay scheme.

2.1.4. Radiolabeling and Radiotracing

Numerous atoms in their elemental form are naturally absorbed, processed and accumulated by the human body, but not all are clinically useful. Radioisotopes of these elements can be used to trace the distribution of certain tissues. For instance, elemental iodine is primarily absorbed by thyroid tissue. Therefore, a gamma emitting radioisotope of iodine like I-123 can be used to image both healthy cells as well as the differentiated thyroid cancerous cells that have metastasized throughout the body [7].

Next, a biologically-relevant molecule can be labeled with a radionuclide. Glucose is one of these molecules; it is the main source of energy for cells throughout the body. Cancerous cells require a lot of glucose to replicate and being able to image glucose metabolism is of definite interest. While it is possible to use Carbon-11 to radiolabel glucose, imaging of Carbon-11 is not practical due to its short half-life [19]. Nevertheless, a surrogate molecule called fludeoxyglucose (FDG) is chemically engineered such that it is indistinguishable from a glucose molecule for the purposes of cellular transport and phosphorylation, while at the same time it can host a positron emitting radioisotope of Fluorine (F-18) characterized by a much more practical half-life of 110 minutes [20].

Another example of a useful molecule is MIBG which is absorbed by neuroendocrine tissues [5]. These tissues are located throughout the body and work in tandem with the nervous system in a feedback loop to release hormones into the bloodstream. The sites of the endocrine system that pertain to this work are the pituitary gland in the central nervous system and the adrenal glands superior to both kidneys. In cases where the aforementioned tissues become cancerous, they can be detected with the help of the MIBG molecule which can labeled with Iodine 123 or Iodine 131. These two radioisotopes decay by gamma ray emission but only I-131 can be used to treat these lesions as it also decays by beta emission.

## 2.2. Imaging modalities

2.2.1. Gamma Camera

Once a gamma emitting radiopharmaceutical is injected into the human body, it is possible to acquire an image that maps out the injected activity as it is absorbed and distributed within different organs or regions of interest in the body. The source of the

gamma rays can be localized by placing detectors on the path of radiation source e.g. a gamma camera in front of a patient who has been injected with a radiopharmaceutical. A clinical gamma camera system has two detector heads each made out of a two-dimensional array of scintillating detectors. The most common configuration of the system is to have one camera posterior and the other anterior to the patient. The array of detectors yields a two-dimensional histogram of all of the gamma rays that traveled perpendicular to the detector i.e. unscattered photons [13].

Measuring the energy of the photons that reach the detector is an essential part of the gamma camera system because energy is an excellent indicator of the aggregate scattering of a photon within matter. For instance, the gamma rays emitted from a given monoenergetic source inside of a phantom would produce a continuous spectrum of energies as a result of multiple scattering events. Moreover, there would be a prominent peak at the known energy of the source. Furthermore, the introduction of pulse height spectroscopy system is vital because it discriminates low energy photons by setting an energy threshold window that encloses the peak [13].

In addition, it would get rid of veil of noise caused by the scattered photons. Although it might seem logical to reduce the size of the energy window in order to improve the spatial resolution of the image, the number of photons detected would be so low that the image produced would not be suited for diagnostic purposes. Furthermore, the amount of signal available is limited by the injected activity, which in most cases would not be increased. Therefore, there is a balancing act between the range of energies accepted by the detector or energy resolution and the sharpness of the source in the final image or spatial resolution [13].

A gamma camera system, shown in figure 2, consists of a collimator, scintillator crystal, light guide, photomultiplier tube array, analog to digital converter (ADC), a computer, and a display [13]. The collimator consists of a lead plate with orifices that only allow unscattered gamma rays to go through. The scintillator converts high energy photons into a proportional number of visible light photons. The light guide is the interface between the crystal and PM tubes. The PM tubes are arranged in an array in order to map out the location of the photons. The analog electrical signal produced in the PM tube is converted into digital signal in the ADC. The digital signal is processed in the computer by making a two-dimensional histogram of the photons within an acceptable range of energies [13].
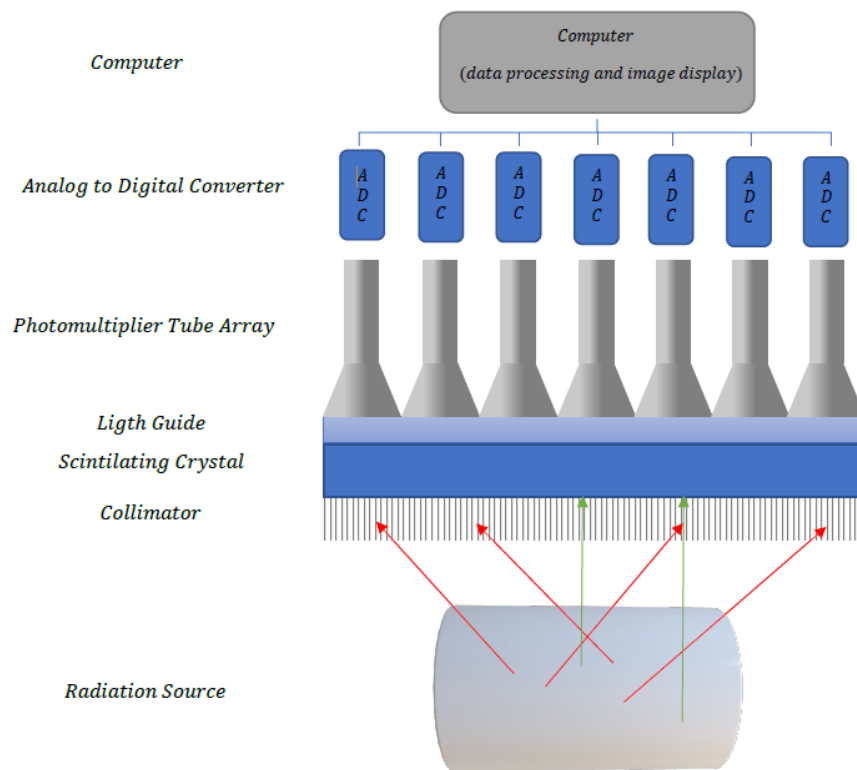
Figure 2.2. Basic diagram of gamma camera system.

2.2.2 Planar Gamma Camera Imaging and SPECT

The gamma cameras can operate in two modes to capture and represent radiation counts. Planar imaging consists of keeping the two gamma cameras in a system in a fixed position, typically one detector posterior and the other one anterior to the patient. The patient is moved within the field of view of the cameras. On the other hand, in Single Photon Emission Computed Tomography (SPECT) imaging the cameras rotate around the patient in order to detect and record the photon being emitted. The rotating aspect of this modality allows for a three-dimensional representation of the emitted photons. While the three-dimensional image is useful in the identification of regions of interest, the time of a full body scan would be unreasonable for patients and it would be prone to more motion artifacts.

2.3. Analyzing Gamma Camera Images

The assessment of images starts by focusing on the areas that contain high amounts of activity and show as high number of counts or areas that are known to be more sensitive to radiation exposure. These areas can be contoured using a processing program, which often come as part of the imaging system or an external software could be used instead. The counts within the region of interest (ROI) can be retrieved through these tools.

The radiopharmaceutical has a known physical half-life in its radioisotope and its biological half-life is dictated by each patient's metabolism [3]. This means that the imaging plan needs to collect data such that the unknow biological half-life can be determined for each patient. Therefore, several scans are needed which might span the length of the average lifetime of the radiopharmaceutical in the human body. The forthcoming sections will present the discussion of how the counts within an ROI are used

to calculate the energy emitted from the ROIs and the energy absorbed by the ROIs in order to estimate a radiation dose to those regions.

2.4. Tracer Kinetic Modeling

This type of modeling adds another dimension to the radiopharmaceutical metabolic process as it aims to assess how the activity concentration changes over time for regions of interest (ROIs) [21]. These types of studies consist of several scans taken over a period of time that fits the physical half-life of the radiopharmaceutical while at the same time capturing the biological half-life of each patient. The biological half-life is evaluated mathematically by having a source of the injected activity present within the field of view of the scans taken. The source is referred to as standard activity and it provides the ability to measure the physical half-life. After the physical half-life is accounted for it is possible to determine the time that the activity spent in each of the ROIs. Furthermore, one can estimate the total residence time of the activity in the ROI, a parameter that is used in the calculation of dose.

2.5. Treating Cancer with Radioisotopes

In the previous sections it was discussed how a radiopharmaceutical can be chemically engineered to target certain types of tissues. The simplest way form of treating cancer with radionuclides is by administering an element that is normally processed by the body. For instance, iodine is taken by the thyroid and its radioactive isotopes like iodine-131 can be used in therapies that treat thyroid cancer. On the other hand, a more complex form of targeting tissues involves molecules created to target certain tissues. An example of this is the molecule Metaiodobenzylguanidine (MIBG) or Iobenguane which is used in neuroendocrine tumor treatments. In fact, it can be used for diagnostic and therapeutic

purposes as it emits both gamma rays and beta particles. The compounds that can be used in this capacity are categorized as theragnostic pharmaceuticals. The most recent development of the MIBG as a theragnostic instrument was made by Progenics Pharmaceuticals. Their protocol, called AZEDRA, was approved for clinical use by the FDA in 2018 [11].

2.5.1. Radiation, Equivalent, and Effective Dose

Radiation dose is defined as the amount of energy absorbed by a unit of mass. The SI units are Joules per kilogram (J/kg) or gray (Gy). However, these units do not convey how different types of radiation ionize matter or how different organs are biologically damaged by radiation. Each type of radiation is assigned a radiation weighting factor (W_R) to represent the severity of the biological damage they cause in tissue. For instance, photons and beta particles both have W_R equal to one, while alpha particles have a W_R equal to twenty. Alpha particles deposit their energy in shorter distances because of their mass and charge. Once the radiation dose is multiplied by its corresponding W_R the quantity is defined as an equivalent dose, with units of Sieverts (Sv). Similarly, each tissue in the human body is assigned a tissue weighting factor (W_T) which represents the radiosensitivity of the tissue. For instance, lung tissue has a W_T equal to 0.12, while liver tissue has a W_T equal to 0.08. The ratios represent the relative radiosensitivity of each tissue because the sum of all the tissue weighting factors must equal unity (1). The dose to individual organs is still referred to as an equivalent dose because at this point only the type of radiation has been taken into account. However, the sum of all tissue weighted organ doses is referred to as an effective dose because it represents the dose to the entire body which also has units of Sieverts (Sv) [22].

2.5.2. External Dosimetry

The dose measurements and calculations from an external source of ionizing radiation to a patient are fairly straightforward due to the known position of the source. Moreover, the images created by the x-ray radiation portray the attenuating/absorption capacity of different tissues. Therefore, the dose to a tissue can be estimated by through the comparison of the known output parameters set before exposure and the measured quantities at the other side of the patient [23].

2.5.3. Internal Dosimetry

Measuring the dose form sources residing inside of specific organs within the body is practically impossible from the standpoint that placing dosimeters inside the patient would require unproductive and invasive surgical procedures to get them in and out of the body. Instead, a purely image-based analysis is needed when dealing with internal dosimetry. Throughout the years, two methods of calculating internal dosimetry have prevailed; these include the classical method and the absorbed fraction method [13]. However, the one that pertains to this work is the absorbed fraction method also known as MIRD named after the institution that came up with it the Medical Internal Radiation Dose Committee of the Society of Nuclear Medicine [24]. The method focusses on the fractions of energy absorbed by different tissues. There are three major calculations that characterize this approach: cumulated activity, energy emitted by the activity, absorbed fraction of energy per unit mass. However, there is a simplified approach to the MIRD method, which only uses the cumulated activity and S-values or dose factors (DF). These values were systematically tabulated through the testing of different radioisotopes in average size

anthropomorphic phantoms [24] [13]. By using these values, the radiation dose can be calculated by ,

$$D = \tilde{A}\, S \qquad (\textbf{Eq.\,2.\,2})$$

where $\tilde{A}$ is the cumulated activity and has units of activity and time $(Bq \cdot s)$, while the S-value has units of dose over activity and time $(Gy/Bq \cdot s)$ [13].

In previous sections, it was discussed how the use of regions of interest helps extract useful information from planar scans. More specifically, the number of counts within an ROI (the amount of activity present in that region) plotted over time (the date and time each scan was taken) yields a time-activity curve. The amount of initial activity decays exponentially with a decay constant given by the physical half-life (T_p) of the radioisotope. However, when the activity is administered to a living being, it does not stay in a single place until it decays completely. Instead it is processed by the body, and at some point, the activity is excreted one way or another. The biological excretion rate is governed by a biological half-life (T_b) of each individual being. Therefore, a combined exponential decay constant is calculated from both physical and biological events happening at the same time or an effective half-life which is given by,

$$T_e = \frac{T_p\, T_b}{(T_p + T_b)} \qquad (\textbf{Eq.\,2.\,3})$$

Additionally, the overall decaying behavior of the activity present can be represented as a function of time that decays with the effective half-life. given by [13],

$$A(t) = A_0\, e^{-\frac{\ln(2)}{T_e} t} \qquad (\textbf{Eq.\,2.\,4})$$

where A_0 is the initial activity administered [13]. Furthermore, integrating the time-activity function with respect to time yields the cumulated activity ($\tilde{A}$),

$$\tilde{A} \approx A_0 \int_0^\infty e^{-\frac{ln(2)}{T_e}t} \, dt$$

$$= \frac{T_e A_0}{\ln(2)} \approx 1.44 \, T_e A_0 \qquad (\boldsymbol{Eq.\, 2.\, 5})$$

where $1.44 T_e$ is the average lifetime or residence time of a radionuclide [13].

After finding the cumulated activity, the dose can be calculated within the ROI by multiplying it with the corresponding S-value. However, this would only correspond to the base case which involves one organ being both the source and target of radiation. The next case and the others after that involve more than two organs which in addition to the step above, the organs also emit radiation towards one another and receive radiation from other organs as well. In fact, the dose reciprocity theorem states that a pair of organs have the same S-value regardless of which organ is the source or target. Having to do this manually would be tedious, thus, software implementations of the simplified MIRD method have been developed.

2.5.4. Software implementation of the MIRD method

In this section, the focus will be guided toward the software used in the methods of this work. It is called OLINDA/EXM® [2] and it can generate the doses to organs by inputting the cumulated activities. Moreover, it provides some customization options. For instance, after choosing one of many available radioisotopes, it is possible to select the type of phantom that better suits the patient complexion; it can also take the specific organ masses of each individual into account. Another useful feature of the program is its unit converter for activity as most people use Curies more often than Becquerels. Figure 2.3 shows the initial window of the program, which displays the aforementioned features. Each of the features will be described further in the next chapter.
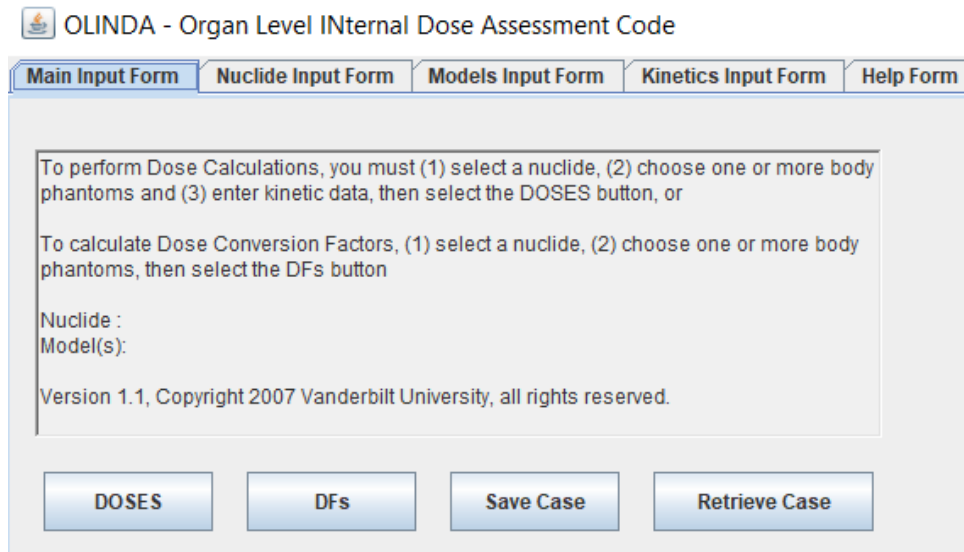
Figure 2.3. Screenshots of different features of the software OLINDA/EXM® version 1.1.

2.6. Therapeutic Injected Activity

2.6.1. Fixed Activities

Radiopharmaceutical therapies are usually prescribed as a function with respect to mass. These fixed activities provide a useful upper bound to avoid hematologic toxicity. Moreover, it was found that the limiting activity to mass ratio is 15 mCi/kg [25]. Furthermore, in a study where patients were treated with high doses (18 mCi/kg) of MIBG I-131 due to a refractory or relapsed neuroblastoma, it was found that hematologic comorbidities were more frequent [12]. Therefore, for an average-size person, who weighs 70 kg, being treated for a neuroblastoma with dose of 15 mCi/kg of MIBG I-131, the limiting activity to avoid hematologic toxicity would be in the order of 1000 mCi. In fact, this is the therapeutic activity upper bound set by the AZEDRA protocol, but at the same time it aims to provide a more patient specific approach by analyzing the activity distribution of each.

2.6.2. Patient Specific Activities

Prescribing dose base on weight might be simple, but it does not provide the most accurate results. For instance, it was found that the prescribing fixed doses do not corelate with the occurrence of hematologic comorbidities, but rather that a dose assessment of a whole-body scan was a more accurate predictor [26]. To further the case for patient specific dose assessments, it is important to consider cases where other organs are at risk of radiation toxicity. In the previous section, it was stated that the AZEDRA protocol sets the 1000 mCi of activity limit, but at the same time it focuses on other organs as well. More specifically, the AZEDRA dosimetry protocol utilizes the dose limits found in the ICRP 118 report [27] for the kidneys, liver, and lungs. Taking these limits into account will allow for a patient specific therapeutic activity prescription. The details of the entire diagnostic and dosimetry processes leading to the therapeutic activity prescription of each patient will be discussed further in the next chapter.

3. Methods and Materials

This chapter will detail the guidelines stipulated by the AZEDRA protocol. For instance, this section will describe the image acquisition, image analysis, and dosimetry calculations. Furthermore, the chapter will go over the features of the external software used to calculate dose to organs by following the MIRD methodology.

3.1. AZEDRA Guidelines

3.1.1. Indications and Diagnosis Guidelines

AZEDRA is a radiopharmaceutical therapy for patients who scan positive for unresectable, locally advanced or metastatic pheochromocytoma or paraganglioma with the Iobenguane Iodine 131 diagnostic scan.

The diagnostic procedure consists of injecting the patient with 5 mCi of AZEDRA which is followed by a set of three scintigraphy planar scans using a gamma camera. The scans aid in the evaluation of the avidity of the tumor, and how the radiopharmaceutical is distributed and cleared over time. There is also a CT scan done to measure the volume (in milliliters) of the organs, more importantly the organs suspected to be at risk. The organ masses are calculated by multiplying the previously obtained volumes and the densities listed in the guidelines for each organ. For instance, the density of the kidneys is assumed to be 1.03 g/cc. Furthermore, in the cases where there is metastasis to the liver and/or the lungs the densities need to be 1.03 g/cc and 0.25 g/cc respectively. The mass of the organs for each patient are used in the dosimetry calculations.

Before the patient is laying on the gamma camera system table, a quality control procedure should be performed for each gamma camera. The quality control procedure should be done by a trained nuclear medicine technologist and set by a certified medical

physicist protocol. Another item that needs to be taken care of before the patient arrives is the preparation of the radiopharmaceutical. The technologists are given specific instructions to prepare both the activity that will be injected and the dosimetry reference standard. The process involves diluting the radioactive Iobenguane solution by using normal saline solution. The activity of the prepared solution should be enough such that it will reach a concentration of 1 mCi/mL by the time it is administered. Therefore, the technologist should to draw 5 mL of solution by using a 10 mL syringe. On the other hand, the standard needs to have an activity of 100 μCi by the time of injection. Since the concentration does not matter in this case, the remainder of the previous solution can be diluted used to create a vile with the aforementioned activity. It is important to note that the standard should not be discarded at any point in the imaging procedure because it will be used for the three scans.

Once the patient arrives, the dosimetric activity and the standard should be residing in a leaded container and ready to use. However, prior to the activity administration, the patient needs to void his/her bladder. Then, the technologist should obtain intravenous access and assure that there is no blockage by administering normal saline solution. Finally, prior to injecting the patient, the activity of the syringe should be measured by using a dose calibrator; the activity should be $\pm$10% from the expected activity. The AZEDRA dosimetric activity should be administered at a steady rate such that the entire process takes 60 seconds.

The first scan occurs one hour after injection. The three scans should be done by the same gamma camera system; the only difference between the exams should be the scanning rate. Furthermore, the reference standard should be placed within the field of view

of the cameras for each of the scans and it should not be touching the patient. For the first scan, the patient needs to be imaged before voiding their bladder. In the case that they need to void, the urine must be collected and imaged in the field of view with the patient. The urine can be discarded after the first scan because for the subsequent scans the patient should void before they are imaged. The second and third scans take place 24 hours and 72 hours later respectively.

The patient should be placed centered and parallel to the scanning axis with their arms to the side to avoid overlap with the organs in the abdomen. The patients should be made comfortable because they will be less likely to move. Once they are positioned correctly, the posterior and anterior images can be obtained for the entire body (top of the heads to the feet) while including the standard. The settings for the scans should be the same: the photopeak of the pulse height spectroscopy system should be set at 364 KeV, the energy window should be 15 percent, the collimator should be set to medium or high energy, and the acquisition matrix should be set to 256×1024. The only setting that should differ between scans is the scanning rate. The scanning rate must decrease for each of the exams because the number of disintegrations per unit time will be decrease at an exponential rate and a certain number of counts are needed to have a useful image. The scanning rate for the first scan is 15 cm/min. Then it decreases by 5 cm/min each time for the subsequent scans i.e. 10 cm/min for the second and 5 cm/min for the third.

3.1.2. Dosimetry Guidelines

The doses to organs are evaluated by extracting data from the images produced by the three scans. There will be a total of 6 images, one posterior and one anterior for each scan. After the last image is acquired, the regions of interest (ROIs) are drawn by the

technologist who took the last image or the physicist in charge of the dosimetry calculations. The ROIs are drawn on the posterior and anterior images taken one hour after injection because the activity can be easily delineated; the ROIs can be copied onto the other scans. The ROIs for the organs start as a polygon shape that encloses the activity hotspot and then the shape can be changed to general shape of the organ. The whole-body ROI is a rectangular shape that encloses the entire anatomy of the patient while excluding the standard of activity. Lastly, the standard ROI is drawn as a circular shape around the standard of activity while making sure that none of the activity coming from the patient is included within the ROI. Thereafter, each image should have seven ROIs: five for the organs (lungs, kidneys and liver), one for the whole body and the last for the standard. Each ROI should be labeled with the number of counts and number of pixels enclosed. The number of counts is recorded for cumulated activity calculations and the number of pixels is recorded to compare the size and shape of the ROI between images. This can easily be achieved by copying the ROI from one image to another. However, in the cases where the software does not allow to copy and paste ROIs, it is a useful parameter to record and evaluate to make sure the areas being evaluated are effectively the same.

The biological half-life or the rate at which the patient processes the radiopharmaceutical will be calculated in the next couple of steps. The first step is to find the mean number of counts detected from the anterior and posterior views for each organ, whole body and standard. More specifically, the geometric mean which is given by,

$$\left(\prod_{i=1}^{n} x_i\right)^{\frac{1}{n}} = \sqrt[n]{x_1 \cdot x_2 \cdot x_3 \cdot \ldots \cdot x_n} \qquad (\boldsymbol{Eq.\,3.1})$$

Therefore, for the case where n =2,

$$\left(\prod_{i=1}^{2} x_i\right)^{\frac{1}{2}} = \sqrt[2]{x_1 \cdot x_2} \qquad (Eq. 3.2)$$

where x_1 is the number of counts in the anterior image and x_2 are the number of counts in the posterior image. The geometric mean provides a central tendency or sense of the most probable number of counts present at a given time. The total number of counts is not needed in this instance because the physical half-life of the isotope is already known for iodine 131 i.e. 8.04 days. The unknown parameter is the biological half-life of the isotope within the patient, which is expected to be different for each patient. The amount of activity present in an ROI is represented as a fraction of total injected activity because the change in activity will be evaluated relative to the initial amount of activity injected. Therefore, the next parameter that needs to be calculated is the percentage of injected activity (%IA). The geometric mean of the whole-body ROIs for the first scan will represent the total amount of activity injected or 100% of injected activity. Therefore, to keep all injected activity accounted for, the first scan needs to happen before voiding. The counts for the other ROIs will be a faction of the total. In the first scan, the counts in each ROI should be divided by the counts in the whole-body ROI. Although the standard is not part of the whole-body ROI it is also represented as a percentage of the total injected activity. The standard should be in the percentage range of 1% and 5%. The expression given in the guidelines is,

$$\frac{GM\ for\ each\ organ}{Whole\ body's\ GM} \times 100 = \%IA \qquad (Eq.\ 3.3)$$

In the second and third scan, the %IA should be multiplied by the standard correction factor, which is given by,

$$\frac{Image\ 1\ Standard\ GM}{Image\ 2\ Standard\ GM} = Correction\ Factor \quad (\boldsymbol{Eq.3.4})$$

This correction factor accounts for the slower scan velocity. Therefore, the %IA for each ROI in the second (2) and third (3) scans is given by,

$$\frac{GM\ for\ each\ Image\ (n)\ ROI}{Whole\ body's\ GM\ for\ Image\ 1} \times Correction\ Factor \times 100 = Corrected\ \%IA \quad (\boldsymbol{Eq.3.5})$$

The next parameter that needs to be recorded is the time. This includes the date and time the activity was injected as well as the three dates and times the scans where acquired. Then, the time difference with respect to the time the activity was injected is calculated for each of the scans. The timestamps and the %IA for each ROI are used to create a time-activity curve. However, when plotting the activity, the percentages need to be converted into ratios by dividing by 100. A mono-exponential curve of activity with respect to time of the form,

$$A(t) = A_0 e^{-\lambda_b t} \quad\quad (\boldsymbol{Eq.\ 3.6})$$

is fitted through the points, where A_0 is the initial activity within the ROI, λ_b is the biological rate of radiopharmaceutical removal. The rate of removal is organ dependent, so there needs to be an individual fit for each organ/ROI. However, the organ pairs can be combined and evaluated as a composite amount of tissue. For instance, the left and right kidney data can be summed into the composite kidneys tissue data.

The next step consists of calculating the cumulated activity from the values obtained from the mono-exponential fit. More specifically, the cumulated activity is the

23

area under the curve and it can be calculated by using Eq. 2.5 and which can be rearranged from being in terms of half-lives to being in term of decay constants,

$$\tilde{A} = \left(\frac{1}{T_b} + \frac{1}{T_p}\right) 1.44\, A_0 = 1.44\, T_e A_0 = \frac{A_0}{\lambda_e} = \frac{A_0}{(\lambda_b + \lambda_p)} \qquad (\boldsymbol{Eq.\ 3.7})$$

where, λ_p is the decay constant given by the physical half-life of iodine 131 i.e. 8.04 days or about 193 hours. Furthermore, since the calculations are done in terms of hours the λ_p can be calculated to be 3.59×10^{-3} events per hour. The last parameter that needs to be calculated is the remainder cumulated activity which is given by,

$$Remainder = whole\ body - \sum(OAR)$$

where, the cumulated activity of all the OARs is subtracted from the cumulated activity of the whole body. The remainder will become useful in the next section where the dose to organs is calculated.

The dose to organs needs to be calculated by a program that implements the MIRD method. Moreover, the program needs to allow for the input of the nuclide being used, the cumulated activities calculated for each tissue of interest as well as the remainder, the patient-specific organ masses, and the amount of activity that will be administered during therapy. The program OLINDA/EXM® has all of these options available and it was the program of choice for determining the dose to organs. In the program, the dose to organs in Gy is determined by setting the amount of activity to 1000 mCi which is the limit activity for hematologic toxicity. Once the doses to organs are obtained, these can be compared to the limiting doses for each organ and limiting injected activity can be determined by,

$$Limiting\ IA\ (mCi) = \frac{limit\ dose\ to\ organ}{calculated\ dose\ to\ organ} \times 1000\ mCi \qquad (\boldsymbol{Eq.\ 3.8})$$

The suggested therapeutic activity will always be less than or equal to the fixed 1000 mCi activity. This means that if the calculated dose to the organ is greater than the limiting dose, the limiting activity will be dictated by that organ and it will be less than 1000 mCi.

3.1.3. Therapeutic Guidelines

The therapy should only be administered to patients that have successfully gone through the AZEDRA diagnostic and dosimetry procedures. Furthermore, the treatment needs to be administered in two doses of 500 mCi or half the calculated limiting activity. This will spread out the activity concentration over time. However, there is still a chance that some side effects will occur. The protocol provides the percentages of people that experienced side effects out of a group of 88 patients: myelosuppression (56%), secondary myelodysplastic syndrome or leukemia (6.8%), hyperthyroidism (3.4%), elevated blood pressure (11%), renal failure (9%), and decrease in glomerular filtration rate (GFR) (22%). Furthermore, there are preventable side effects such as fatal pneumonitis, which occurred one time 9 weeks after a single treatment. Also, embryo-fatal toxicity can be avoided by taking the necessary precautions. Lastly, infertility can be temporary or permanent for some patients. Another notable aspect to highlight is that 12% of patients discontinued the treatment after experiencing adverse reactions.

3.2. OLINDA/EXM®

This section will explore the different features of the OLINDA/EXM® version 1.1 software. First, once the program is installed and opened, the window in figure 3.1 pops-up and the instructions on how to use the program need to be followed to calculate dose to organs. Each step listed can be carried out on by going into the different tabs of the program. For instance, the first step is on the next tab, shown in figure 3.2, and consists of

choosing the element as well as the isotope of that element that is being used. In this case the isotope is iodine-131. The next tab, shown if figure 3.3, has several options to choose from in terms of the type of body that the patient might have. Then, the last tab in the program, shown in figure 3.4, gives the user the opportunity to enter the cumulated activity for the source organs. The numbers entered in the figure are not actual patient data, but are there to show which cells would be filled with the cumulated activity from the dosimetry calculations discussed in the previous section. Namely, the cells of the kidneys, liver, lungs and the remainder are the ones that would be filled in this case.

Once these parameters are entered, the user needs to return to the main input form tab and click on the 'DOSES' button. This will open a new window, shown in figure 3.5, where more parameters can be entered for a patient specific dose calculation to the organs at risk. In the new window, the user can press the 'Modify Input Data' button and begin to change the masses of organs obtained from the CT volumes. The total mass of the patient can be changed, but it did not have any effect in the final dose to each organ. To apply the changes to the calculation, the user needs to click on the 'Done' button and the doses to the organs will be recalculated. The final step, shown in figure3.7, is to enter the maximum therapeutic activity that would be delivered, i.e. 1000 mCi. This is done by entering the activity in mCi and then pressing the 'convert' button to calculate the activity with units of MBq. Lastly, the user needs to press the 'Mult. Doses by (MBq)' button and the final doses to organs will be calculated. The doses calculated are in units of mSv and can easily be converted to doses in mGy because the types of radiation have a radiation weighting factor of 1.
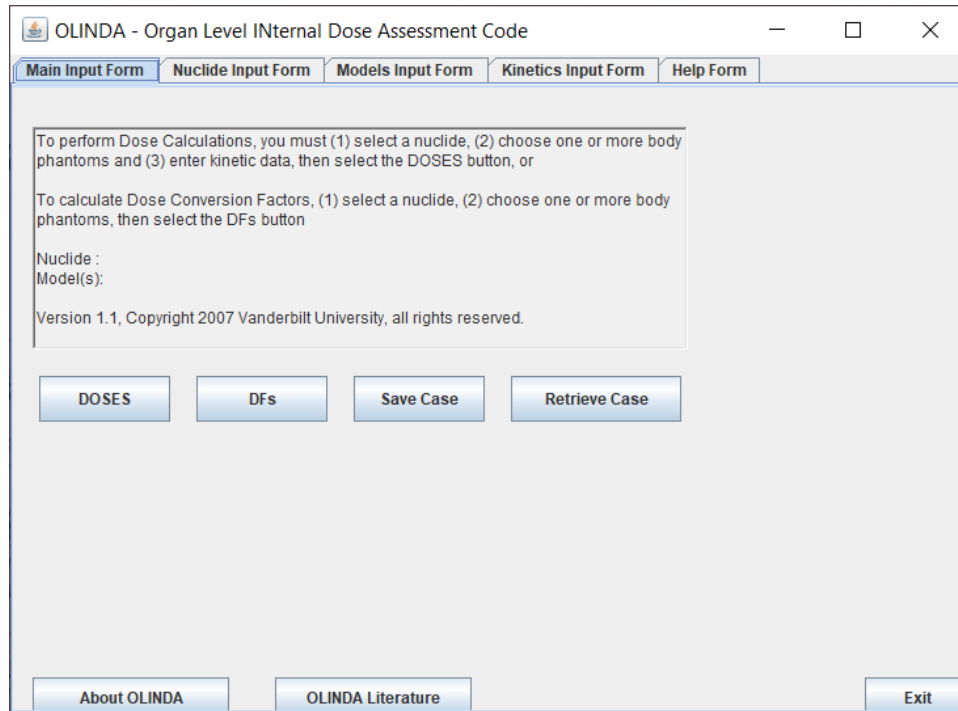
Figure 3.1. Initial window of the program OLINDA/EXM®.
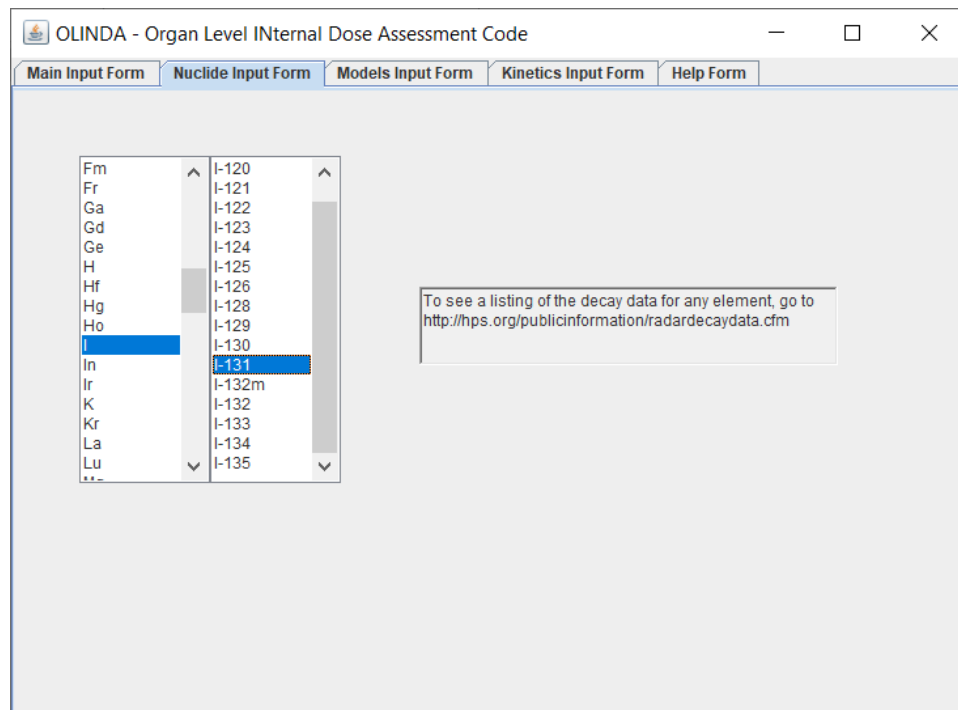
Figure 3.2. Nuclide input form tab in the OLINDA/EXM® program that allows the user to select the isotope that will deliver dose.
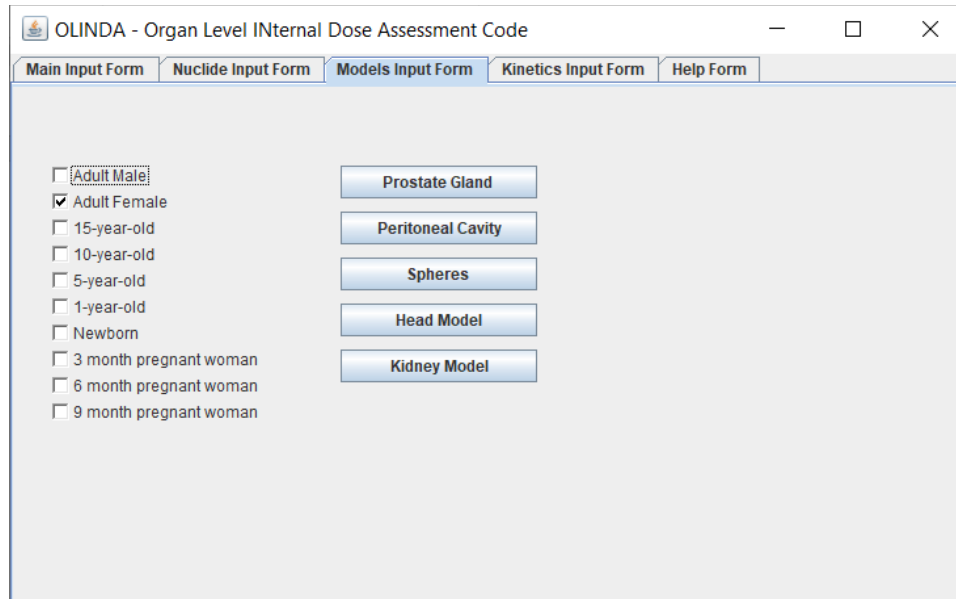
Figure 3.3. Model input form tab in the OLINDA/EXM® program allows the user to select the phantom that better fits the complexion of the individual being evaluated.
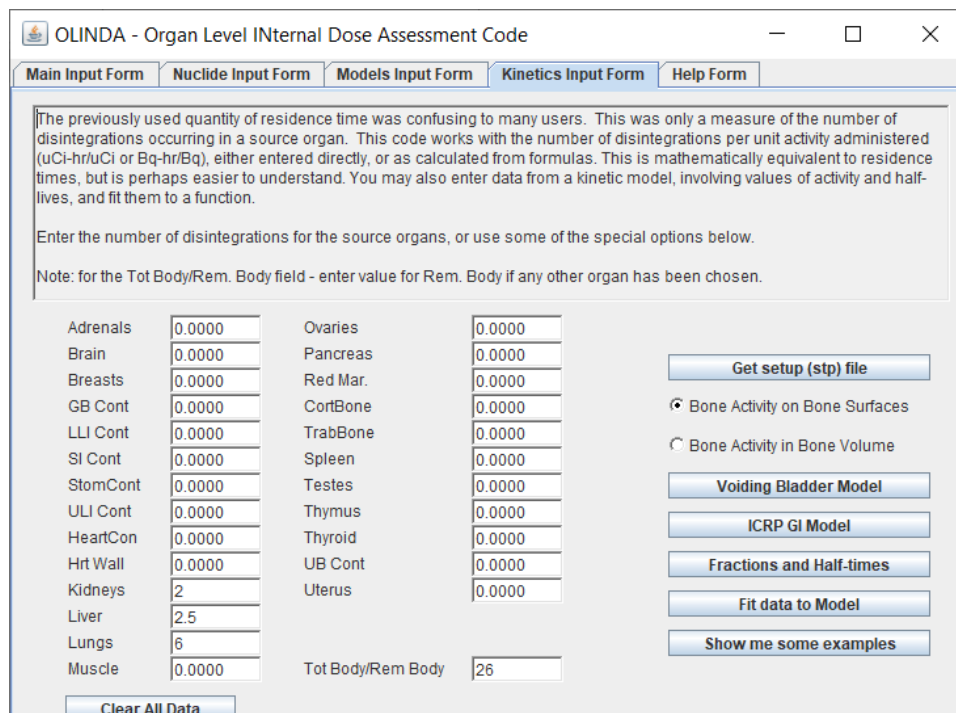
Figure 3.4. Kinetics input form tab in the OLINDA/EXM® program allows the user to enter the cumulated activity for the source organs and the remaining cumulated activity residing in other parts of the body. The values entered have units of Bq-hr/ Bq.
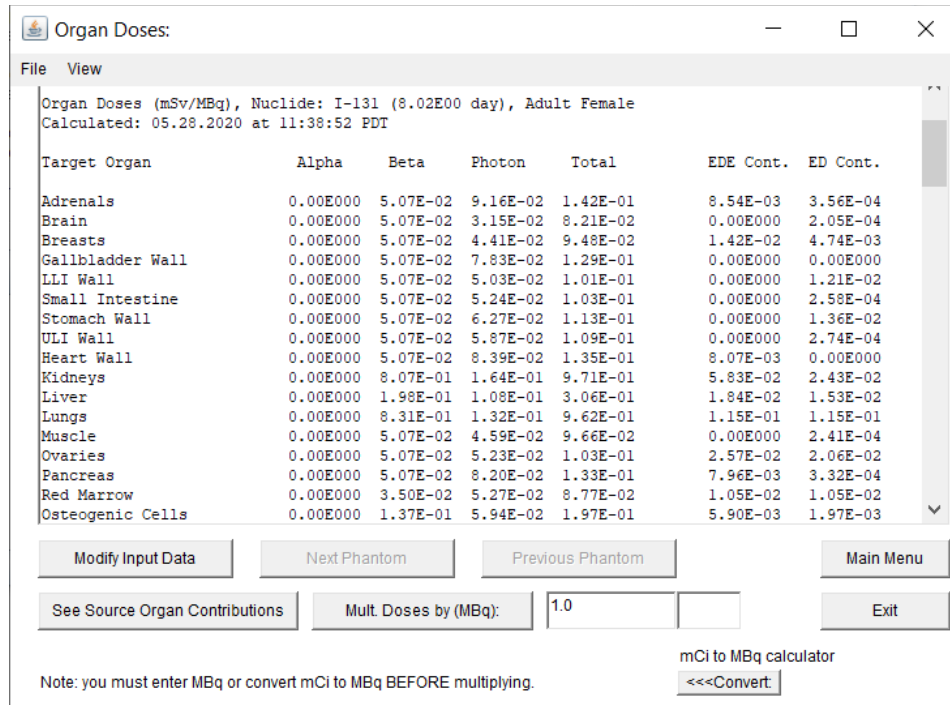
Figure 3.5. New window that opens after the 'DOSES' button is pressed in the main input form tab shown in figure 3.1.
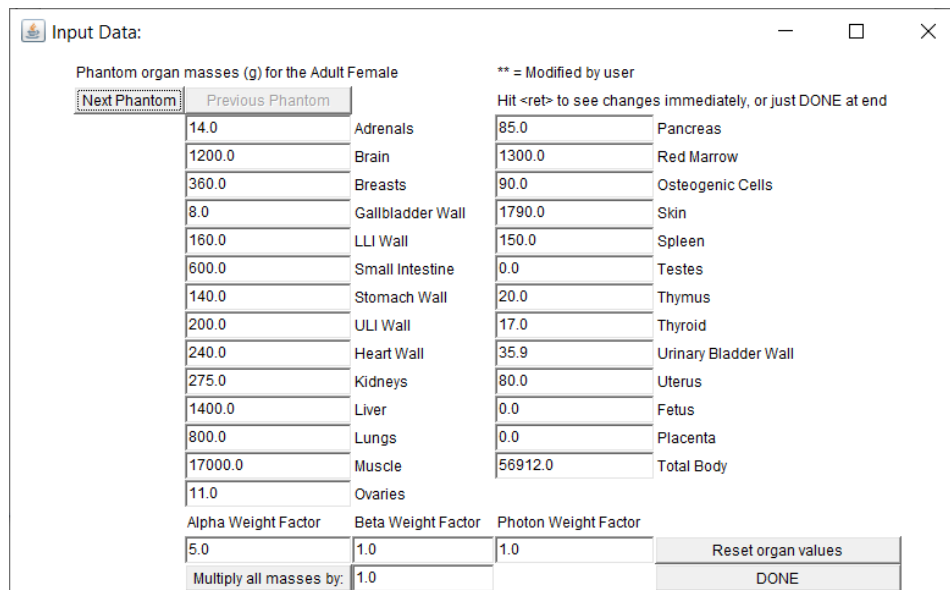
Figure 3.6. New window that opens after the 'Modify input Data' button is pressed in the window shown in figure 3.5. The masses to organs can be changed to the masses obtained from the CT volumes of the individual being evaluated. Any changes will be applied by pressing the 'DONE' button.
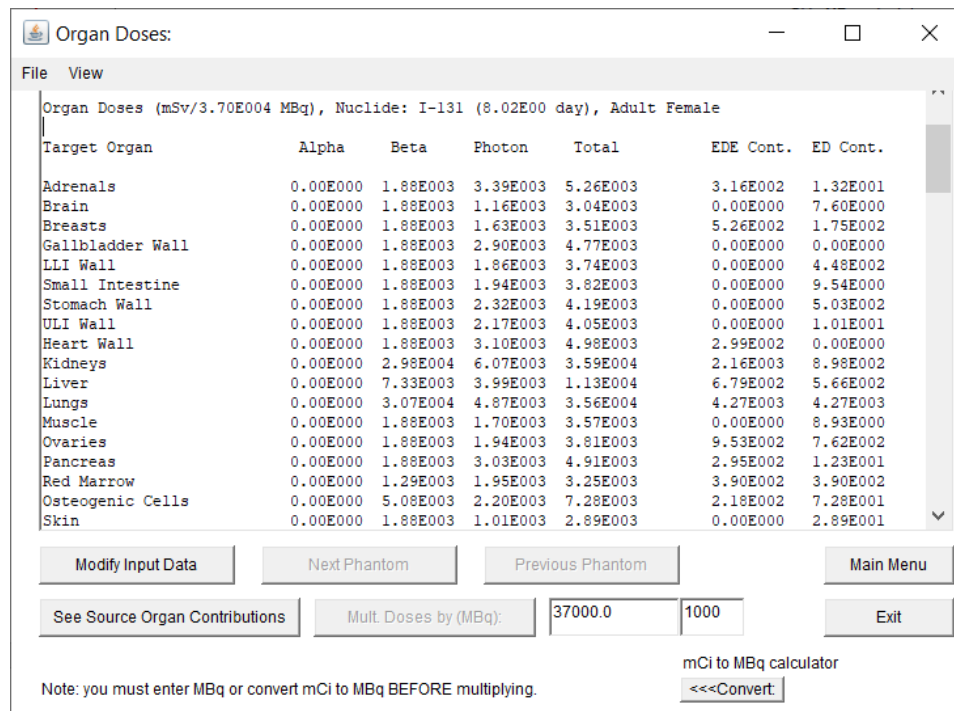
Figure 3.7. The doses to the organs in mGy are calculated by pressing the 'Mult. Doses by (MBq)' can be done after entering the activity being used with of mCi and converting it to an activity with units of MBq.

4. Results

This chapter will describe the implementation of dosimetry protocol detailed in the previous chapter. At the same time, this section will describe how the tool was used to assess the data from two patients, who were then treated at OHSU with the AZEDRA therapy.

4.1. Results from Image Analysis

The number of counts and number of pixels were extracted from each of the images. For instance, in figure 4.1 the ROIs for the kidneys were drawn and labeled with the number of counts and the number of pixels. The ROIs were drawn for the first posterior image, taken one hour after the injection, and then copied onto the next images. Furthermore, the ROIs for the anterior view were mirrored and adjusted to fit the general shape of the activity hot spots or general position of the anatomy.
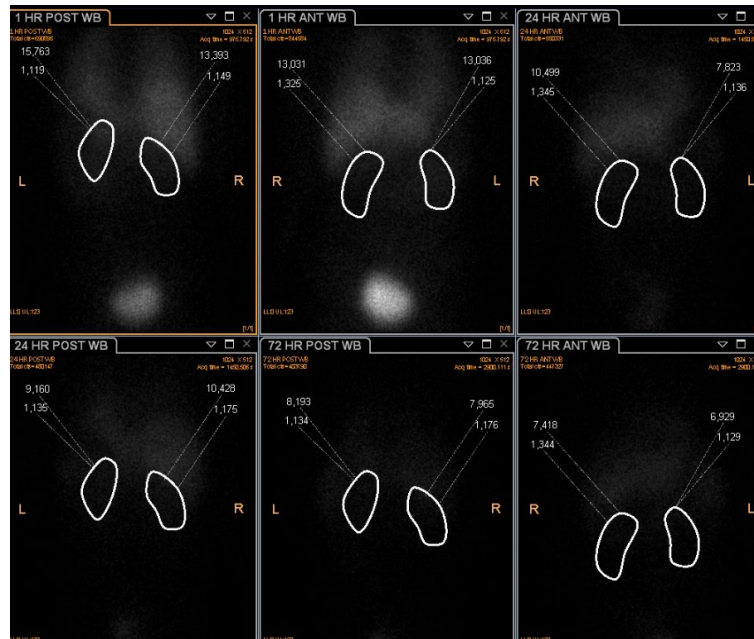
Figure 4.1. Regions of interest drawn onto the anterior and posterior scintigraphs taken over the span of three days.

Next, the data from the images is organized into a table. Table 4.1 shows the number of counts and pixels for each ROI. It also shows the pixel coefficient of variance which is calculated to ensure that the regions of interest are virtually the same shape and cover the same area. In the table, the cells highlighted with green are blank for the user to fill with the pertinent patient data and the cells highlighted with yellow are auto filled every time a row is completed.

Table 4.1. Recorded number of count and pixels for each ROI drawn in the scintigraphs. Calculated variance between the number of pixels assures that the shape and size of the drawn ROIs are on par with other ROIs that measure the same area.

Date/Time	1/1/2020	14:38	1/2/2020	14:21	1/4/2020	14:06	
ROI Name	Counts	Pixels	Counts	Pixels	Counts	Pixels	Pixel COV (%)
Kidney L Ant	13,036	1,125	7,823	1,136	6,929	1,129	0.493%
Kidney L Post	15,763	1,119	9,160	1,135	8,193	1,134	0.794%
Kidney R Ant	13,031	1,325	10,499	1,345	7,418	1,344	0.842%
Kidney R Post	13,393	1,149	10,428	1,175	7,965	1,176	1.312%
Liver Ant	108,258	4,085	65,843	4,166	41,916	4,178	1.221%
Liver Post	88,576	3,799	51,246	3,871	30,603	3,865	1.039%
Lung L Ant	24,867	2,391	13,499	2,443	9,279	2,430	1.118%
Lung L Post	31,097	2,588	17,893	2,631	12,096	2,628	0.918%
Lung R Ant	26,886	2,501	17,174	2,557	11,157	2,553	1.231%
Lung R Post	34,514	2,408	16,446	2,457	10,055	2,460	1.196%
Standard Ant	16,639	1,694	22,970	1,770	37,010	1,768	2.484%
Standard Post	20,098	1,739	27,723	1,770	44,277	1,767	0.972%
Whole-body Ant	821,735	253,814	519,980	258,440	395,204	258,160	1.010%
Whole-body Post	663,357	254,727	442,779	259,082	339,916	259,082	0.976%

4.2.   Results from Dosimetry Calculations

The first set of calculations involves taking the difference between the acquisition times and the initial injection time. Table 4.2 displays the date and time for the different events in the imaging process, however, the dates were switched for patient anonymity. Then the time difference is calculated and recorded in terms of hours. These time

differences will be used to plot the time-activity curves in the next couple of steps. Another parameter that is recorded within this table is the gamma camera's velocity for each scan with units of centimeters per minute (cm/min). The velocity should not change between patients, so the information is purely for reference. This table should be programed to be auto filled by entering the date and time values in the table 4.1.

Table 4.2. Time record of the different events and the time difference in hours for each of the events with respect to the time the injection was administered. The camera's velocity is displayed for reference for each of the scans. The velocity decreases to account for the lower activity expected as time passes.

Date	Time	Event	Δt (hr)	Camera Velocity (cm/min)
1/1/2020	13:51	Injection	NA	NA
1/1/2020	14:38	Scan1	0.78	15
1/2/2020	14:21	Scan2	24.50	10
1/4/2020	14:06	Scan3	72.25	5

The next set of calculations map out the biological behavior of the activity within each of the ROI over the span of the three scans taken. The first set of calculations are the geometric mean given by equation 3.2, and the percentage of injected activity (%IA) given by equations 3.3-3.5. Alternatively, the geometric mean can be calculated in excel through the formula 'GEOMEAN'. In table 4.3 the calculated geometric mean and calculated %IA for each of the images are calculated and displayed. Similar to the last couple of tables, the calculations can be automated by populating the cells with their respective formulas. The table also provides identifying parameters of elapsed time from the injection for each of the images, which were calculated in table 4.2.

Table 4.3. Geometric mean and percentage of injected activity for each ROI over the span of the three scans.

	Image #1		Image #2		Image #3	
	Elapsed Time (hr)		Elapsed Time (hr)		Elapsed Time (hr)	
	0.78		24.50		72.25	
Source Organ	**Geo Mean**	**%IA**	**Geo Mean**	**%IA**	**Geo Mean**	**%IA**
L Kidney	14335	1.94%	8465	0.83%	7535	0.46%
R Kidney	13211	1.79%	10463	1.03%	7687	0.5%
Liver	97924	13.26%	58088	5.70%	35816	2.19%
L Lung	27808	3.77%	15541	1.53%	10594	0.65%
R Lung	30462	4.13%	16806	1.65%	10592	0.65%
Standard	18287	2.48%	25235	2.48%	40481	2.48%
Whole Body	738311	100.00%	479829	47.10%	366519	22.4%

The next couple of tables in the analysis tool, namely tables 4.4 and 4.5, take the calculated percentages of injected activity from the last table (4.3) and present these values as fractional amounts of injected activity instead. In both tables, each image is identified with its respective time elapsed since the injection. These tables have the same information, the only difference between them is the fact that in table 4.5 the amount of activity is consolidated for the pairs of organs i.e. kidneys and lungs.

Table 4.4. The fraction of injected activity in each of the regions of interest.

Time (hr)	L Kidney	R Kidney	Liver	L Lung	R Lung	Whole Body
0.78	0.01942	0.01789	0.1326	0.0377	0.0413	1.000
24.50	0.00831	0.01027	0.0570	0.0153	0.0165	0.471
72.25	0.00461	0.00470	0.0219	0.0065	0.0065	0.224

Table 4.5. The fraction of injected activity in each of the tissues at risk of radiation toxicity.

Time (hr)	Kidneys	Liver	Lungs	Whole body
0.783333	0.03731	0.1326	0.0789	1.000
24.5	0.01858	0.0570	0.0317	0.471
72.25	0.00931	0.0219	0.0130	0.224

The next steps help visualize and determine the exponential decay of activity present within the ROIs by plotting a time activity curve and fitting a mono-exponential curve through the points respectively. For instance, the biological decay within the combined ROIs of the kidneys from one of the patients is shown in figure 4.2. The figure also displays the function fitted through the points, which is of the form described by equation 3.6. The R^2 value is also displayed and it represents how well the function conforms to the data points i.e. the proportion of variation in the activity that can be attributed to the uncertainty in the time points recorded. The uncertainty comes from the fact that the activity is collected over a period of time, but it is represented in the graph as a single point in time. Ultimately, these parameters provide the means to calculate the cumulated activity or area under the curve, which will be used to calculate the dose to the organs at risk in the next section.
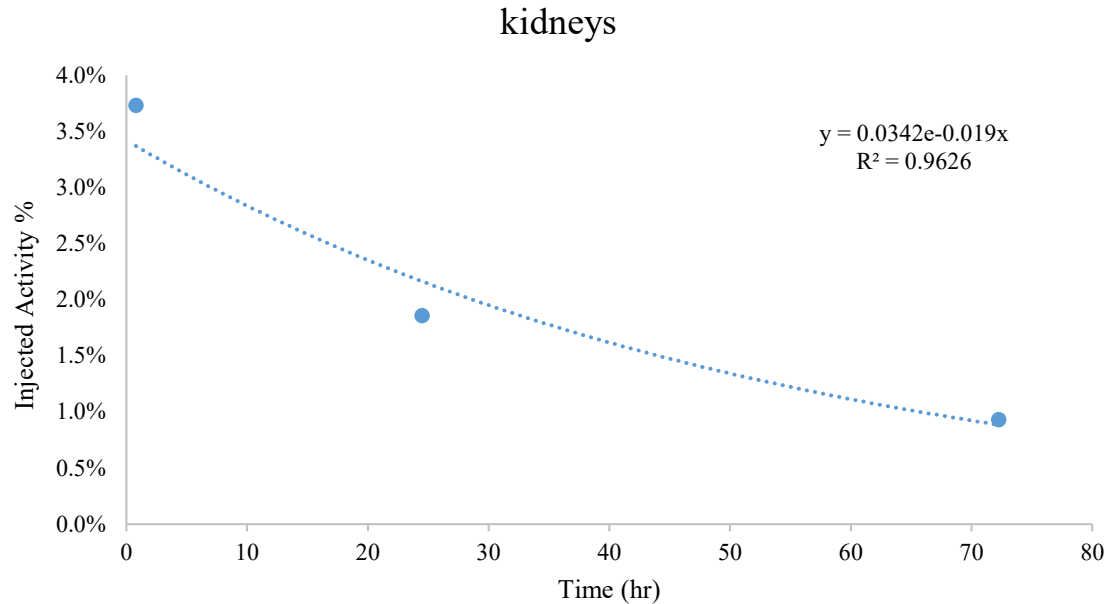
Figure 4.2. Mono-exponential curve fitted through the decaying amount of activity present the combined ROIs of the kidneys. In this case the initial activity is about 3.8% with respect to the total activity of the whole body and after three days it decays down to just under 1%.

Although, visualizing the data can be useful. It is more practical to create a table where the parameters and resulting cumulated activity are displayed after being calculated. Namely, table 4.6 shows the analytical exponential regression of the time activity data. The formula used in excel is 'LINEST' which is a linear regression formula, but it can be modified to be an exponential regression by setting taking the natural logarithm of the y-value i.e. the percent injected activity. The results of this formula are displayed in two cells. As shown in table 4.6, the negative biological decay constant ($\lambda - value$) is displayed followed by the natural logarithm of the initial activity. The latter value can be converted into the initial activity by evaluating the value with the exponential function i.e. $EXP(\ln(A))$ in excel. The last calculation is done by using equation 3.7, where the calculated initial activity and biological decay constant along with the known physical decay constant for iodine 131 are used to calculate the cumulated activity.

Table 4.6. Mono-exponential regression of the time-activity data and the calculated cumulated activity for the different organ tissues and whole-body regions of interest.

ROIs	-λ-value (/hr)	ln(A)	A-value	Cumulated Activity (MBq-hr/MBq)
kidneys	-0.018703347	-3.37546	0.034202	1.534048
liver	-0.024446797	-2.10696	0.121607	4.33708
lungs	-0.024335482	-2.65376	0.070386	2.52029
whole body	-0.02014173	-0.09448	0.909845	38.33523
remainder	-	-	-	29.94381

4.3. Results from OLINDA/EXM®

The next step in the procedure takes place outside of the analysis tool, namely in the program OLINDA/EXM®. The pertinent information can be selected for each patient by following the detailed guide on the program in the previous chapter (section 3.2). The initial doses can be calculated after inputting the radioisotope being used, the type of patient complexion as well as the cumulated activity, which was calculated in the previous section. Then the doses to organs can be modified by changing the mass of the organs to the patient specific masses shown in table 4.7 and setting the activity that will be evaluated.

Table 4.7. Organ masses calculated from the volumes obtained from a CT scan of the patient and the density of the organs set by the AZEDRA dosimetry protocol.

	Total Volume from CT (ml)	Density from protocol (g/ml)	Total organ mass (g)
Kidneys	292	1.03	301
Liver	1400	1.03	1440
Lungs	1990	0.25	800
Whole body	-	-	6230

OLINDA/EXM® provides the contributions to dose from the different types of radiation as well as the total dose to the target organ. The calculated doses to the organs at risk can be extracted onto a table in the analysis tool, i.e. table 4.8.

Table 4.8. Doses to organs at risk calculated in the program OLINDA/EXM®, separated by the beta and gamma contributions that make up the total dose deposited onto each of the organs.

Target Organ	Beta contribution (mGy)	Gamma contribution (mGy)	Dose (mGy)
Kidneys	1.05E+04	2.51E+03	1.30E+04
Liver	6.18E+03	2.62E+03	8.80E+03
Lungs	1.04E+04	2.21E+03	8.08E+03

4.4.   Therapeutic Activity Calculation Results

The last set of calculations involve the use of the previously obtained organ doses (table 4.8) and the limiting organ doses set in the ICRP report 118. In table 4.9, both the calculated and limiting doses are displaced. Furthermore, there is an extra column showing the dose from 500 mCi which is listed as a reference because the treatment itself takes place in two sessions where half of the prescribed activity is delivered in each session. Lastly, the table also shows the limiting injected activity which is calculated by using equation 3.8.

Table 4.9. Calculation of the limiting injected activity by comparing the calculated dose to the organs when using the fixed activity of 1000 mCi and the limiting dose to the organ set by the ICRP report 118.

Injected Activity(mCi)→	500	1000	Limiting Doses (Gy)	Limiting IA (mCi)
Organs at Risk	Calculated Doses (Gy)			
Kidneys	13.00	26	23	884.62
Liver	8.80	17.6	30	1704.55
Lungs	8.08	16.16	17.5	1082.92
Maximum allowable activity (mCi) →				**884.62**

5. Discussion

In the previous section, the details of the tool implementation were described while at the same time the patient data was shown throughout the different tables created for data organization and automated calculations. Therefore, in this chapter the focus will be aimed towards analyzing how different results from the dosimetry protocol calculations affect the patient at several levels. Next, the different types of cancer treatments will be compared and contrasted. Then, the aspects that make the AZEDRA therapy patient specific will be looked at further. Additionally, the effective dose that the AZEDRA therapy has on the patient population will be calculated and analyzed. Finally, the implications of imaging during treatment will be touched upon to discuss its possibility.

5.1. Therapeutic Activity Prescription and Patient Outcome

There is a lower and an upper bound for the injected therapeutic activity. The physician in charge as well as the physicist doing the dosimetry calculations need to be aware of the draw backs and benefits of prescribing therapeutic activities near the upper and lower bounds. The lower bound is set as the minimum activity prescribed which will spare the vast majority of healthy tissues while ablating a fraction of cancerous cells. In the best-case scenario, the cancerous cells will be ablated such that the cancer becomes remissive. On the other hand, the worst-case scenario, the majority of the cancer cells will be ablated, but there will remain enough cells for it recur.

To combat the latter, many cancer treatments focus on eliminating the cancerous cells first and then focus on reducing the dose to healthy tissues by coming up with different treatment plans, which is more than reasonable to do. In chemotherapy, it is done by attacking the cancer on a regular basis over a set period of time. Similarly, radiation therapy

plans can span over several weeks to keep attacking the cancer consistently while letting the healthy tissue recover. Therefore, it is unadvised to stop treatment before finishing all sessions because the cancer, though slower than normal cells, can recover as well. Furthermore, the radiation therapy plans often rely on inverse planning to achieve the desired tumor coverage and if there is normal tissue burden, the plans can be improved through iterations. The plans are changed until the tumor can be treated successfully and the surrounding tissues are safe. The AZEDRA therapy, and many of the other chemically engineered radiopharmaceuticals for that matter, do not require dosimetry measurements/calculations for the tumors is because these molecules target cancerous cells at a much higher rate than normal/healthy tissues. For instance, the MIBG molecule will target the neuroendocrine cells because it binds to the norepinephrine transporters. This allows for the treatment plan to prioritize the burden caused to the healthy tissues of the radiation dose from the therapeutic activity.

Now, the upper bound is dictated by the radiation toxicity of normal/healthy tissues. In the case of iodine 131, the hematologic toxicity is the main concern as it needs preemptive preparation to treat these comorbidities. Furthermore, the limit was found through the trials of fixed activities base on weight. In fact, it was found that in their last increment of 3 mCi, at 15 mCi per kg of activity were enough to start seeing hematologic problems [25]. Furthermore, there is also evidence for more extreme cases were tested, where 18 mCi per kg were injected to patients with refractory or relapsed neuroblastoma. These cases always resulted in a hematologic problem after treatment.

Lastly, the cases in between are the ones discussed in this work, where the upper bound is set and the focus is on other boundaries set for other organs at risk. For instance,

the maximum allowable therapeutic activity in the case shown in table 4.9 was below the fixed rate, namely 885 mCi as a total therapeutic activity. This case in particular shows how the kidneys were the limiting organ of the therapeutic activity. In the other case, not shown, the organs processed the radiopharmaceutical at a faster rate and the activity did not spend as much time in the organs. However, it is not only a matter of how much time the activity spends in the organ, the size and mass of the organ also plays a role in these calculations as dose is a function of energy deposited onto mass. However, it is important to note that there is an aspect that can be overlooked, which is the uniformity of activity distribution. In this protocol implementation it was assumed that the activity was evenly distributed although, there is times where if there is significant tumor burden in the lungs or the liver the density changes. The density chosen in the protocol for liver (1.03 g/ml) concurs the literature where it can vary from 1.017 g/ml to 1.077 g/ml [28]. The density recommended for lungs (0.25 g/ml) also concurs with the literature where the density during inspiration is between (0.21 g/ml) and 0.26 (g/ml) [29]. Furthermore, as previously mentioned, the dose prescribed stops at 1000 mCi because of hematologic toxicity rather than following the lowest calculated activity for the kidneys, liver, or lungs during the dosimetry process.

5.2. Generalizations in the AZEDRA Protocol

There are some generalizations that can be seen as limitations of the protocol; however, these limitations are heavily bound to the standards deemed reasonable by the FDA for clinical use. Nevertheless, discussing how these generalizations are reasonable for clinical use is important. At the same time, it is important to discuss how other

alternatives would change the outcome/results of the dosimetry calculations and if these alternatives would be worth implementing.

5.2.1. Activity Homogeneity within ROIs

In this work, it is assumed that the injected activity distributes throughout the organ/ROI homogeneously, however this is not the case. This can be observed in figure 4.1, where the (most noticeable) activity in the lugs is not distributed homogeneously in the lung tissue. This is not characteristic of the AZEDRA protocol itself, but any type of image analysis that deals with ROIs. Making this assumption is not only time effective, but it is the most conservative approach. It is time effective because one does not have to dive deeper into the intricacies of the all ROIs. Furthermore, it is a conservative approach form the perspective that a hotspot only affects a small volume of the organ, which would be preferable for the organ's functionality. The functionality of an organ can be maintained even when a fraction of the organ volume is compromised [30]. In other words, a section of an organ can be irradiated until the cells are no longer viable and section that was not irradiated can still perform the functions of the organ. Each organ has its own whole and fractional limits, but ultimately the organ as a whole is more radiosensitive than a fraction of that organ. Moreover, the limits set in the ICRP report 118 are based on the dose to the whole organ.

5.2.2. Mono-exponential Fit

Another generalization that is made in the protocol is that the distribution and biological processing of the radiopharmaceutical over time within each organ follows a mono-exponential trend. However, there is a buildup region when the radiopharmaceutical is being distributed within the organ. Therefore, it would be reasonable to argue for a fit

that describes this upward trend is needed for a complete description of the events. Nevertheless, it is important to notice the time scale at which the events are happening. For instance, the distribution/uptake of the radiopharmaceutical happens within a couple of hours. This assessment can be made from the fact that there is a significant decrease in activity within the ROI between the one-hour scan and the 24 hours scan i.e. the peak activity was reached sometime within that interval of time. More importantly, the next event happens 72 hours after the injection and the activity has decreased but it has not reached zero yet. This means that the peak was reached within a couple of hours while the biological procession of the radiopharmaceutical is still happening after three days. Therefore, characterizing the time-activity curve as mono-exponential, i.e. only describing the biological decay of the radiopharmaceutical, is not only fair description of what is happening in the larger time scale, but it can be easily modeled.

5.2.3. Dealing with Organ Overlap

The protocol provides an appendix section within their dosimetry protocol for the instances where there is a gross overlap between two of the organs at risk in planar imaging. For instance, the overlap of the liver with the right kidney. The protocol suggests that the percentage injected activity of the left kidney, and the ratio of the right and left kidney masses obtained from the CT volumes should be used to calculate the percentage injected activity for the right kidney.

Another way of dealing with overlap issues is by using SPECT imaging instead of planar imaging. This would be a more involved procedure for the patient because a whole-body SPECT would be needed in order to perform the necessary dosimetry. However, this method has other advantages such as fusing the SPECT data with the CT data. Fusing these

data is beneficial because the contouring of organs becomes more accurate due to the clear distinguishable boundaries between organs in the CT scan.

5.3. Advantages of Radiopharmaceutical Therapy

At the begin, the three main approaches to treat cancer were introduced. Moreover, it was stated that radiopharmaceutical therapies are a hybrid of chemotherapy and external beam radiation therapy. Now, it is important to emphasize the ways by which this option for treating cancer is advantageous over others. For instance, it is advantageous in cases where there are not solid tumors. An external beam treatment plan can target easily target a volume of cancer that has macroscopic boundaries. However, it becomes difficult to 'aim the beam to a target' so to speak, if there is not a clear target. Therefore, in the cases where not only the boundaries between cancerous tissue and normal tissue are microscopic, but there might be metastatic developments, radiopharmaceutical therapy is better equipped to find and treat these sorts of cancerous tissues. This is due to the fact that these radiopharmaceuticals are chemically engineered to target specific kinds of tissues. In the case of the AZEDRA therapy, the radiopharmaceutical is able to target neuroendocrine tissues by biding to the neurotransmitters within these types of cells. This is the exact reason why the dosimetry protocols of these types of treatments are centered around sparing dose to the healthy tissue rather than targeting the tumor itself.

5.4. Patient Specific Traits

There are two main traits within the AZEDRA dosimetry protocol that make the final therapeutic activity prescription a patient specific guided assessment. These two traits deal with the intrinsic definition of dose i.e. energy deposition on mass. For instance, the dosimetry calculations done for this therapy take into account the amount of energy

deposited onto the organs at risk. This is done because the uptake and biological processing of radiopharmaceuticals varies from one patient to another. The second trait is the mass of the organs at risk. The mass of each OAR is obtained from the CT volumes and the density of the organ provided in the dosimetry protocol. Furthermore, the measured organ masses are used in the OLINDA/EXM® to substitute the masses of the phantom selected. The assessment of individual organ mass is particularly important because mass is inversely proportional to the dose deposited. For instance, if the organ masses are not changed during dose calculation it would mean that if the patient's organ mass is smaller than the organ mass in the phantom, the dose to the organ would be larger and vice versa. The former being of particular concern because assessing patients with phantom data would lead to the prescription of a therapeutic activity that surpasses the dose limits of the organ at risk.

5.5.   Effective Dose Assessment

The effective dose to the whole body can calculated by summing the dose to each of the organs and scaling the dose with each tissue weighting factor. However, it is important to note that effective dose should not be used to assess risk on an individual level [31]. Instead it can be used to assess how a treatment affects the patient population being treated. The program OLINDA/EXM® calculates the effective dose as part of the organ dose calculations. For instance, in the case discussed in the results section where 884.62 mCi were administered, the effective dose was 5.8 Sv. On the other hand, for the case where 1000 mCi were administered, the effective dose was 6.6 Sv. Although, the 1000 mCi activity is the upper bound of the activity being prescribed, there can be a slight variation in the resulting effective dose as the biological processing of the radiopharmaceutical or

the organ masses change in a patient to patient basis. Nevertheless, one can start to see a general range of effective doses for this treatment.

5.6. Imaging During Treatment

Imaging how the activity is distributed throughout the body during treatment would help rectify the dose calculations done during the diagnostic and dosimetry procedures. Furthermore, it would help identify other organs that might be at risk. However, there are several limitations that do not allow patients to be imaged during treatment. First, there needs to be a controlled environment for the high activity that these patients carry with themselves during treatment. For instance, a patient could be injected with 500 mCi of activity in one therapy session. Additionally, the current technology is not capable of imaging these high activities because the detectors have a dead time after each count is registered. Therefore, some counts would not be detected, and there would be a constant stream of photons being detected. A viable option to consider is to image the patient near the end of treatment as the activity would be much lower. However, this would still need heighten safety precautions because of the potentially high activity. Therefore, it would be worth calculating the point in time during the treatment the activity is low enough to be imaged.

6. Conclusions

The data analysis tool developed from this research allows for straightforward, patient-patient specific treatment of neuroendocrine tumors. Once imaging for a patient is completed, one can obtain the counts from the regions of interest and input them into the tool. The cumulated activities are then calculated automatically and can be used in the OLINDA/EXM® program along with the organ masses and the limiting activity of 1000 mCi to obtain the doses to the organs at risk. The last step of the process requires the input of the calculated organ doses back into the analysis tool, at which point, the maximum allowable therapeutic activity is calculated.

By using patient data for the dosimetry calculations, the prescribed therapeutic activity accommodates each patient individually. In fact, the tool has proven to be clinically useful in determining dose estimates to the kidneys, liver and lungs of two patients who have already been successfully treated. In these two patients it was possible to see how different one patient can be from the other because one was given a reduced activity while the other was given the fixed limiting activity due to their different metabolisms of the radiopharmaceutical. The implementation of this image analysis and dosimetry tool allows for a streamlined performance of patient-specific organ dose estimation, and therapeutic activity calculation.

References

[1] Progenics Pharmaceuticals, "AZEDRA Iobenguane 131 solutions for intravenous use," Tarrytown, NY, 2018.

[2] M. G. Stabin, R. B. Sparks and E. Crowe, "OLINDA/EXM: The Second-Generation Personal Computer Software for Internal Dose Assessment in Nuclear Medicine," *Journal of Nuclear Medicine,* 2005.

[3] Y. Chai-Hong, C. Mu-hua and N. Kwan-Hoong, "Therapeutic radionuclides in nuclear medicine: current and future prospects," *Journal of Zhejiang University Science B,* vol. 15, no. 10, 2014.

[4] V. Rufini and B. Shulkin, "The evolution in the use of MIBG in more than 25 years of experimental and clinical applications.," *Italian Association of Nuclear Medicine (AIMN) [and] the International Association of Radiopharmacology (IAR), [and] Section of the Society of Radiopharmaceutical Chemistry and Biology,* no. 52, pp. 341-50, 2009.

[5] I. Ilias, C. Divgi and K. Pacak, "Current role of MIBG in the diagnosis of pheochromocytoma and medullary thyroid cancer," *Seminars in nuclear medicine,* vol. 41, pp. 364-8, 2011.

[6] C. Jimenez, W. Erwin and B. Chasen, "Targeted Radionuclide Therapy for Patients with Metastatic Pheochromocytoma and Paraganglioma: From Low-Specific-Activity to High-Specific-Activity Iodine-131 Metaiodobenzylguanidine," *Cancers,* vol. 11, no. 7, 2019.

[7] H. Hupf, J. Eldridge and J. Beaver, "Production of Iodine-123 for medical applications," *The International Journal of Applied Radiation and Isotopes,* pp. 345-351, 1968.

[8] B. F. Hutton, "The Origins of SPECT and SPECT/CT," *European Journal of Nuclear Medicine and Molecular Imaging,* 2014.

[9] K. Gupta and Sandeep, "Calculation of the Range of Electrons for parts of Human Body over the Energy Range of 30 – 1000 KeV," 2015.

[10] Washington State Department of Health, "Iodine 131 (I-131) Fact Sheet 320-085," 2003.

[11] Food and Drug Administration, "FDA approves first treatment for rare adrenal tumors," U.S. Department of Health and Human Services, 2018.

[12] S. G. DuBois, J. Messina, J. M. Maris, J. Huberty, D. V. Glidden and J. Veatch, "Hematologic Toxicity of High-Dose Iodine-131–Metaiodobenzylguanidine Therapy for Advanced Neuroblastoma," *Journal of Clinical Oncology,* vol. 22, no. 12, 2004.

[13] S. R. Cherry, J. Sorenson and M. Phelps, Physics in Nuclear Medicine, Elsevier Inc., 2012.

[14] United States Environmental Protection Agency, "Radioactive Decay".

[15] M. Berger, J. Coursey, M. Zucker and J. Chang, "Stopping-Power & Range Tables for Electrons, Protons, and Helium Ions," ational Institute of Standards and Technology (NIST), 2017.

[16] P. L. Olive, "The Role of DNA Single- And Double-Strand Breaks in Cell Killing by Ionizing Radiation," *Radiation Research,* 1998.

[17] W. J. Cannan and D. S. Pederson, "Mechanisms and Consequences of Double-strand DNA Break Formation in Chromatin," *Journal of Cellular Physiology,* 2016.

[18] W. Aljubeh, A. Shaheen and O. Zalloum, "Radioiodine I-131 for Diagnosing and Treatment of Thyroid Diseases," 2012.

[19] E. Ehrin, N. S. Stone-Elander, J. L., M. Bergström, G. Blomqvist, T. Brismar, L. Eriksson, T. Greitz, P. E. Jansson, J. E. Litton, P. Malmborg, M. Ugglas and L. Widén, "C-11-labeled Glucose and Its Utilization in Positron-Emission Tomography," *Journal of Nuclear Medicine,* 1983.

[20] S. Yu, "Review of 18F-FDG Synthesis and Quality Control," *Biomedical Imaging and Intervention Journal,* 2006.

[21] S. Huang, "Role of Kinetic Modeling in Biomedical Imaging," *Journal of Medical Sciences,* vol. 28, no. 2, pp. 57-63, 2008.

[22] International Commission on Radiological Protection, "ICRP Publication 103. The 2007 Recommendations of the International Commission on Radiological Protection," ICRP, 2007.

[23] X. G. Xu, B. Bednarz and H. Paganetti, "A review of dosimetry studies on external-beam radiation treatment with respect to second cancer induction," *Physics in medicine and biology,* 2008.

[24] W. Bolch, K. Eckerman, G. Sgouros and S. Thomas, "MIRD Pamphlet No. 21: A Generalized Schema for Radiopharmaceutical Dosimetry—Standardization of Nomenclature," *The Journal of Nuclear Medicine,* vol. 50, no. 3, pp. 477-484, 2009.

[25] K. Matthay, K. DeSantes, B. Hasegawa, J. Huberty, R. Hattner, A. Ablin, C. Reynolds, R. Seeger, V. Weinberg and D. Price, "Phase I dose escalation of 131I-metaiodobenzylguanidine with autologous bone marrow support in refractory neuroblastoma.," *Journal of Clinical Oncology,* vol. 16, no. 1, 1998.

[26] S. Buckley, S. Chittenden, F. Saran, S. Meller and G. Flux, "Whole-body dosimetry for individualized treatment planning of 131I-MIBG radionuclide therapy for neuroblastoma.," *Journal of Nuclear Medicine,* vol. 50, no. 9, 2009.

[27] ICRP, "ICRP Publication 118. ICRP Statement on Tissue Reactions / Early and Late Effects of Radiation in Normal Tissues and Organs – Threshold Doses for Tissue Reactions in a Radiation Protection Context," ICRP, 2012.

[28] B. A. Overmoyer, C. E. McLaren and G. M. Brittenham, "Uniformity of Liver Density and Nonheme (Storage) Iron Distribution," *Arch Pathol Lab Med,* 1987.

[29] E. Kohda and N. Shigematsu, "Measurement of Lung Density by Computed Tomography: Implication for Radiotherapy," *Keio Journal of Medicine,* 1989.

[30] E. J. Hall and A. J. Giaccia, Radiobiology for the radiologist (Seventh edition), Philadelphia, PA: Wolters Kluwer Health/Lippincott Williams & Wilkins, 2012.

[31] D. R. Fisher and F. H. Fahey, " Appropriate Use of Effective Dose in Radiation Protection and Risk Assessment," *Health Physics,* vol. 113, no. 2, pp. 102-109, 2017.